Hydrogen generator integrated with fuel cell for portable energy supply

Journal of Physics: Energy

PAPER

Hydrogen generator integrated with fuel cell for portable energy supply

V Yartys[1], I Zavaliy[2,*], V Berezovets[2], Yu Pirskyy[3], F Manilevich[3], A Kytsya[2], Yu Verbovytskyy[2], Yu Dubov[2] and A Kutsyi[3]

[1] Institute for Energy Technology, Kjeller 2027, Norway
[2] Karpenko Physico-Mechanical Institute of the NAS of Ukraine, 5 Naukova St., 79060 Lviv, Ukraine
[3] Vernadskii Institute of General & Inorganic Chemistry of the NAS of Ukraine, 32/34 Acad. Palladina Prosp., 03142 Kyiv, Ukraine
* Author to whom any correspondence should be addressed.

E-mail: ihor.zavaliy@gmail.com

Keywords: $NaBH_4$ hydrolysis, Pt catalyst, fuel cell, portable energy supply

Supplementary material for this article is available online

OPEN ACCESS

RECEIVED
1 July 2022

REVISED
2 December 2022

ACCEPTED FOR PUBLICATION
13 December 2022

PUBLISHED
29 December 2022

Abstract

An autonomous power supply device based on a 30 W fuel cell (FC) stack and a hydrolysis-type hydrogen generator was developed. The creation of this device included the construction of a unit for hydrogen generation, development of an electronic control unit for the operation of the device, and testing and optimizing the overall performance. The hydrolysis of $NaBH_4$ was catalyzed by Pt-based catalysts and was studied for different reactor configurations and reagent concentrations. The flat type of the reactor, Pt catalyst deposited on cordierite as a support, and 10% solution of $NaBH_4$ proved to be the most efficient when generating H_2 for use in the 30 W FC. A developed electronic control unit effectively regulates the hydrolysis reaction rate and provides the required hydrogen supply to the FC. A Li-ion battery was used to start the work of the developed system. One important feature of the developed electronic system is the use of supercapacitors, enabling smoothening of the periodic variations of the generated power. The created hydrolysis unit integrated with the FC provides a stable power supply for at least 9 h from one refueling (U_{const} = 12 V, I = 0–2.5 A, nominal power = 30 W). The specific generated power of the system when accounting for its weight and volume is similar to the analogues described in the reference data, while the electronic circuit enables its stable and efficient performance, satisfying the consumer needs for autonomous energy supply when a stationary electrical grid is not available.

1. Introduction

An efficient portable energy supply should meet such requirements as high specific weight efficiency and limited noise of operation, in addition to improved fuel efficiency, long operation time and broad operation temperature range. The most effective portable energy supply systems contain a chemical hydride-based fuel cell (FC) system, and are suitable for various applications [1, 2]. An FC with a simple configuration operates using hydrogen as a fuel and oxygen as an oxidizer. It has high energy density and efficiency as electrical energy is directly generated by an electrochemical reaction. Furthermore, the FCs are safe, reliable, eco-friendly, do not emit any noise and provide vibration-free operation. Among the known methods of obtaining hydrogen for the FC supply, the hydrolysis of energy-storing [3] or energy-accumulating [4] substances (binary and complex metal hydrides (MgH_2, $NaBH_4$, $LiBH_4$ and others), light metals (Al, Mg) or their alloys) deserves special attention, as hydrogen can be generated directly at the place of its use, which allows the challenges associated with its production, storage and transportation to be bypassed [3–6].

The strategic energy roadmaps of many countries envisage the use of hydrogen to address energy availability. These plans include the development of hydrogen production, fueling station infrastructure, FCs

and FC vehicles [7]. In the further development of proton exchange membrane fuel cells (PEMFCs), the main efforts will be devoted to highly active, durable and cheap catalysts to generate H_2 at a sufficient rate [8].

The catalytic hydrolysis reaction of sodium borohydride ($NaBH_4$) [3] is one of the most promising methods of generating pure hydrogen directly at the place of its use [3, 9, 10]. In alkaline solutions, the interaction of $NaBH_4$ with water practically does not proceed at ambient conditions, which allows such solutions to be stored for a long time. However, in the presence of various homogeneous or heterogeneous catalysts, the hydrolysis of borohydride actively proceeds at room temperature with the formation of hydrogen and sodium metaborate:

$$NaBH_4 + 2H_2O \rightarrow NaBO_2 + 4H_2. \quad (1)$$

The theoretical gravimetric hydrogen storage capacity of $NaBH_4$ is 10.8 wt.% [3]. Hydrogen yield after the completion of the hydrolysis of 1 kg of $NaBH_4$ is 2367.7 l (normal conditions) or 211.4 g.

The most active metal catalysts in the reaction (1) are nanodisperse rhodium, ruthenium and platinum, in particular, when immobilized on various substrates [3, 9, 10]. Their activity depends on the conditions of reduction and immobilization of the metals, the nature of the used precursors, the amount and dispersity of the reduced metals, and the type of substrate. Among the other catalysts, the main attention of researchers is devoted to non-noble metals such as nickel and cobalt, due to their low cost and high efficiency [11–15]. That is why our efforts were also directed towards the synthesis and investigations of the activity of nanostructured Ni/Co-based catalysts with different structures and compositions. For example, the calculated activation energy of the hydrolysis reaction in the presence of $Ni_{50}Co_{50}$ was only 26 kJ mol^{-1} (the lowest value in comparison with the reference data). Then, accounting for the high specific rate of hydrogen generation (1600 ml per 1 g of catalyst per 1 g of $NaBH_4$ at maximum) as well as the linear kinetic curve of H_2 evolution, spanning a range up to ~90% of $NaBH_4$ conversion, $Ni_{50}Co_{50}$ nanoparticles may be considered as a prospective material for use in portable and stationary applications [16].

Despite numerous publications on hydrogen generation from $NaBH_4$ for FCs, only a limited number of papers have described the pilot (hydrogen generators and power systems) devices [17–27]. Below, we will briefly review some of them.

Kojima *et al* [17] developed a hydrogen reactor containing a Pt-$LiCoO_2$-coated honeycomb cordierite monolith, which provided a maximum H_2 generation rate of 120 ml min^{-1}. It was used to feed a specially designed 10 kW H_2/air PEM FC. Gervasio *et al* [18] reported a small reactor to feed a 10 W FC. For this purpose, they used a 30 wt.% solution of $NaBH_4$ in 4 wt.% NaOH, and Ru/Al_2O_3 was used as a catalyst for hydrogen generation.

Kim *et al* [19] developed a novel reactor integrated with a 450 W PEM FC stack. The main system consists of five parts aimed at generating hydrogen, retrieval of the spent fuel, product cooling, gas–liquid separation and H_2 purification. The optimal hydrogen generation system enabling operation of an FC was implemented using a Co-B/Ni foam catalyst with a flow rate of 17.5 ml min^{-1} of aqueous solution comprising 20 wt.% $NaBH_4$ and 1 wt.% NaOH. The working processes were controlled electronically.

A few years later, Kim *et al* [20, 21] designed and fabricated an FC system for application as a power source for unmanned aerial vehicles. It consisted of three major parts: an FC stack, a hydrogen generator and a hybrid power management system. The standard power output of the FC stack was 80 W. The hydrogen generator comprises a fuel cartridge, a micro pump, a catalytic reactor, a gas–liquid separator and a dehumidifier. An operating hydrogen rate of 1071 ml min^{-1} was provided by the hydrolysis of 15 wt.% $NaBH_4$ and 5 wt.% NaOH using the Co/Al_2O_3 catalyst. The same pellet-shaped catalyst and aqueous solution of 20 wt.% $NaBH_4$ were used to design a hydrogen generator for the 200 W PEM FC stack [23]. In order to reduce the volume and weight of the entire FC system, Kim [24] proposed a fuel tank integrating a $NaBH_4$ solution tank and a $NaBO_2$ solution tank. He also designed a small catalytic reactor for the hydrolysis of $NaBH_4$ based on the Co-B coated porous ceramic material ISOLITE, which is composed of Al_2O_3 and SiO_2, and has a porosity of 71%. A 100 W FC stack in this system was also modified by replacing heavy aluminum components with acryl parts.

Li and Wang [26] developed a powerful hydrogen generation system for the operation of the 3 kW PEM FC. It consisted of a 2.5 l stainless steel batch reactor, a heat exchanger with four 4 W fans, a 10 l buffer tank, a 5 l plastic fuel tank and a control module. Cobalt oxide with nickel foam was used as a catalyst for the hydrolysis of the 15 wt.% solution of $NaBH_4$. A simulation model was proposed, which allowed adjustment of the model parameters based on the experimental data, while a batch control algorithm was developed to adjust the batch intervals when the PEM FC load was varied. Batch control was implemented by using a microcontroller and integrating it with a PEM FC for the experimental validation.

In the papers [25, 27–29], the authors proposed a new hydrogen generator using a solid-state sodium borohydride as a hydrogen source. An acid solution could be injected onto the solid $NaBH_4$ to accelerate the

hydrolysis without the use of a catalyst. The required amount of gaseous hydrogen was obtained by using hydrochloric acid via the reaction $NaBH_4 + xHCl + (x + a + 2)H_2O = xNaCl + xH_3BO_3 + (1-x)$ $NaBO_2 + aH_2O + 4H_2$. A solution of 3–4 M HCl was selected to obtain the maximum hydrogen yield. The reactor enabling excess operating pressure was an important feature for achieving stable system operation. The generated hydrogen was temporarily pressurized in the reactor and was supplied to the FC on demand. The hydrogen supply system was successfully designed and integrated with a 100 W FC. The authors proposed a mechanism that allows a stable hydrogen supply to the FC. Furthermore, they developed a movable fuel cartridge and redesigned the injection device.

As shown in the reviewed articles, the autonomous power supply devices can be created by combining FCs with hydrogen generators, in which the catalytic hydrolysis of $NaBH_4$ is carried out. The nano-dispersed metal (noble and non-noble) catalysts for $NaBH_4$ hydrolysis immobilized on the surface of solid substrates were applied. Various designs, catalysts and modes of operation of hydrogen generators were proposed, which define the performance characteristics of the FC utilizing hydrogen fuel. To ensure stable operation of an autonomous power source, an automatic control system for hydrogen generation is required to account for the load of an FC.

In the present study, platinum catalysts immobilized on several substrates were prepared, and the regularities of $NaBH_4$ hydrolysis on such catalysts in flow-through flat and cylindrical reactors were investigated. The most effective immobilized platinum catalyst was used in the proposed flow hydrogen generator. An electronic control system for the management of the operation of a power source based on the FC battery and hydrogen generator was developed. A prototype of a portable autonomous power source, including a 30 W FC stack, hydrolysis-type hydrogen generator and electronic control system, was manufactured and validated.

2. Materials and methods

The kinetics of $NaBH_4$ hydrolysis in the presence of catalysts were investigated in a volumetric setup, the main components of which were cylindrical or flat flow reactors with catalysts and a eudiometer or a SmartTrak® M100L flowmeter by SIERRA. The reactors were made of acrylic resin. The borohydride solution was pumped through the reactors using a peristaltic pump. The generated hydrogen was passed through a moisture trap. The volumes of hydrogen evolved, collected and measured in the eudiometer were converted to normal conditions. The rate of hydrogen evolution, measured by a flowmeter, was recalculated into the volume of released hydrogen using special software.

Platinum catalysts were prepared by their deposition on various substrates. Nanodisperse platinum was applied to Vulcan XC-72 carbon black (up to 40 wt.%) using a $H_2PtCl_6 \cdot 6H_2O$ solution and sodium borohydride as a reducing agent. The synthesis was carried out in an alkaline solution of ethylene glycol and formaldehyde. To control the particle size, polyvinylpyrrolidone additives were used. At a concentration of 0.2%, the size of the platinum nanoparticles was 2–3 nm, and with an increasing content of polyvinylpyrrolidone to 0.6%–1.2%, the particle size decreased to 1.5–2 nm.

To prepare a nanodisperse platinum catalyst immobilized on carbon cloth, a catalytic ink, including platinum catalyst Pt (40%)/Vulcan XC-72 and 30–50 wt.% of 5 wt.% dispersion of Nafion D521 monomer on an alcohol base 1100 EW, was prepared by ultrasonic treatment at a frequency of 22–25 kHz for 2–3 min. The resulting ink was applied to plain carbon cloth (trademark 1071 HCB) by spraying with an airbrush followed by intermediate drying to achieve a mass of platinum catalyst of 1–2 mg cm^{-2}. Samples of the carbon cloth applied with the catalytic ink layer were heat treated at 130 °C and then placed into a reactor.

The polyol-synthesis with reduction by $NaBH_4$ was used to deposit a nano-dispersed platinum on the activated granular carbon AG-3. The prepared composite catalyst contained 75 mg of platinum per gram of activated carbon.

Platinum was electrochemically deposited from the electrolyte containing 25 g l^{-1} of K_2PtCl_6, 100 g l^{-1} of $NaNO_2$ and 20 ml l^{-1} of ammonia solution (0.915 g cm^{-3}) at a temperature of 70 °C at a cathode current density of 20 mA cm^{-2} on porous, defatted and etched titanium crumb. Under these conditions, the yield of platinum was about 30%. The weight of precipitated platinum was monitored gravimetrically. The surface density of the platinum was 1–4 mg cm^{-2}.

The nanodisperse platinum catalyst immobilized on the surface-modified cordierite (Pt/Al_2O_3/cordierite) was prepared according to the procedure described in [30]. Commercial synthetic cordierite (general formula $2MgO \cdot 2Al_2O_3 \cdot 5SiO_2$) of honeycomb structure with a square canal density of 400 canals per square inch and a canal cross-sectional area of 1 mm^2 was surface-modified by Al_2O_3 sol, and then nanodisperse platinum was applied. The main steps of the preparation procedure were the preparation of the sol for the modification of the cordierite surface by alumina, formation of the alumina layer on cordierite, and application of the active component (Pt) to the surface-modified cordierite. After the

modification of the cordierite surface by Al_2O_3 sol, the substrate was impregnated with H_2PtCl_6 solution. For the reduction of platinum, a 10% $NaBH_4$ solution was used. The content of platinum in the prepared composite catalyst was 27.9 mg g^{-1}.

3. Results

3.1. Studies of $NaBH_4$ hydrolysis reaction and selection of the effective catalysts

The obtained kinetic curves of hydrogen generation during the hydrolysis of 10% $NaBH_4$ water solution containing 5% NaOH and 50 mg platinum catalyst on carbon black XC-72 at 25 °C are presented in figures 1(a) and (b). It can be seen that after the initial period of the process, hydrogen evolves steadily and evenly. The self-heating of the reaction mixture was negligible.

The measured rate of hydrogen evolution during the hydrolysis of 10% $NaBH_4$ + 5% NaOH solution at 24 °C in a flat flow reactor with a nanodispersed Pt catalyst immobilized on the carbon cloth was directly proportional to the pumping rate of the solution and reached 400 ml min^{-1} at a $NaBH_4$ solution flow rate of 7.8 ml min^{-1} (figures 2(a) and (c)). This is sufficient for a stable supply to the 30 W hydrogen–oxygen FC with hydrogen used as a fuel. The extent of decomposition of sodium borohydride decreases with the increasing rate of pumping of the solution through the generator. Moreover, the platinum catalyst immobilized on carbon cloth was less active in the cylindrical reactor than in the flat one due to the catalyst particles peeling off from the cloth during the formation of the roll.

It was found that the platinized titanium is less active than the catalyst obtained by the polyol method (figures 2(b) and (d)). It appeared that a continuous platinum film was formed on the titanium surface, and this film was less efficient as a catalyst than nanodispersed platinum deposited on other substrates.

The nanodisperse platinum catalyst immobilized on the surface-modified cordierite was the most active and reliable. The rate of hydrogen evolution during the hydrolysis of $NaBH_4$ on such catalyst was practically constant at a constant concentration of $NaBH_4$ and the flow rate of its solution (see figure 3). As the rate of the solution flow increased, the hydrogen evolution was accelerated. The prepared catalyst provided a high and stable rate of hydrogen generation upon moderate heating of the $NaBH_4$ solution (65 ± 5 °C) [31]. In addition, as shown in [32], the creation and use of such composite catalysts made it possible to avoid the aggregation and/or entrainment of nanodisperse platinum particles by the $NaBO_4$ solution flow, which helps to preserve the catalyst activity during long-term operation. The nanodisperse platinum catalyst immobilized on the surface-modified cordierite was chosen for the decomposition of $NaBH_4$ alkaline solution in the flat flow reactor, which was part of the developed prototype of a portable power supply device.

3.2. Hydrogen generator with platinum catalyst immobilized on a cordierite carrier and design of a portable power source

The cordierite block with dimensions of 60 × 24 × 12 mm was used to prepare the monolithic Pt-containing catalyst as described above. The catalyst was placed into a flat flow reactor made of acrylic resin (see figure 4).

The scheme and appearance of the autonomous power supply device are shown in figures 5 and 6, respectively. The device includes the following main components: FC stack, hydrolysis reactor with a composite catalyst, tank with fresh 10% $NaBH_4$ + 5% NaOH and waste solutions, hydrogen dehumidifier, pump and electronic control system. The tank consists of two reservoirs, one for the fresh alkaline solution of $NaBH_4$ and another for the waste solution. The tank also serves as a liquid–gas separator for separating hydrogen from the waste solution.

The tank is made of acrylic resin, and silicone tubes are used to carry the solution and hydrogen gas. To supply the solution to the reactor, where the hydrolysis reaction takes place, a 12 V RS385-635peristaltic pump from Intlab is used. When $NaBH_4$ alkaline solution is pumped through the reactor, the hydrolysis reaction of $NaBH_4$ takes place on the catalyst surface with the generation of hydrogen and $NaBO_2$. The formed reaction products are transferred to an appropriate reservoir of the tank, where a separation of hydrogen from the solution occurs. The wet hydrogen then passes through a trap with a Drierite® dehumidifier (98% $CaSO_4$ + 2% $CoCl_2$, Hammond Drierite Ltd.). The dried hydrogen enters into a PEM FC stack operating with air cooling. A 30 W PEM FC (FCS-B30) from Horizon FC Technologies was used. The operation of the pump and the FC stack is controlled by an electronic control unit. The generated electricity is then supplied to the consumer. The size of the device is approximately 125 mm × 100 mm × 350 mm.

The hydrolysis of 1.1 l of 10% $NaBH_4$ + 5% NaOH solution ensures the operation of a 30 W FC for 9–10 h at a consumed current of 3.6 A and an output voltage of 8.4 V. In this case, the flow rate of hydrogen, formed in the generator, is at least 0.42 l min^{-1}. The maximum operating temperature of the FC battery is 30 °C, and that of the hydrogen generator is up to 70 °C. The operation temperature is limited to the temperature range for the FC, and is 5 °C–30 °C. The changes in the operational temperature window can be achieved by applying temperature control using heating or cooling (this, however, was outside the scope of

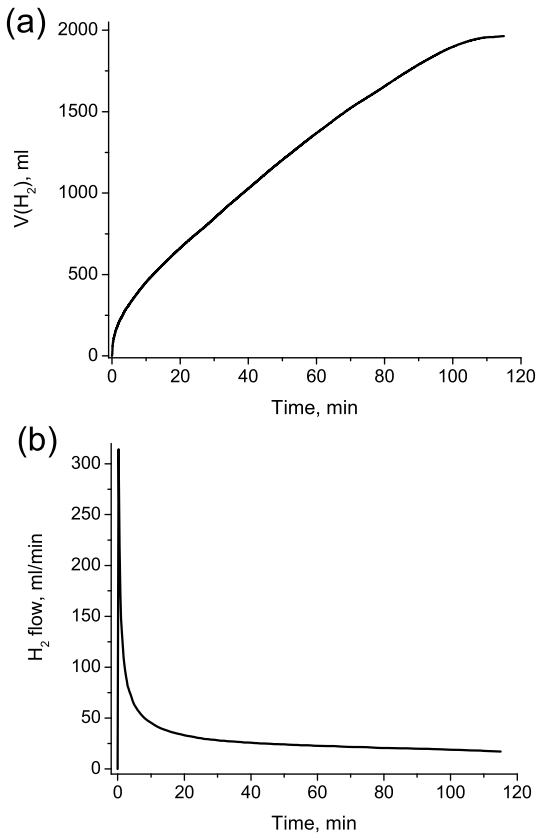

Figure 1. Kinetic curves of hydrogen evolution at 25 °C from 10% $NaBH_4$ solution containing 5% NaOH and 50 mg of catalyst Pt (40%)/XC-72.

the present work). At temperatures lower than room temperature, the device will remain less efficient until the reactor warms up. During the start-up, a sufficiently high amount of borohydride solution will be supplied to provide the required supply of borohydride ions, while the concentration of the BH_4 ions decreases during the operation. We note that the performance of the present device is limited by the freezing temperature of the used solution. This can be overcome by additional heating of the container for hydrolysis. At low temperatures, another challenge is the decreased solubility and the increased viscosity of the solution of the reaction products. Under such conditions, it is necessary to reduce the concentration of borohydride or to employ additional heating of the pipeline between the reactor and the container with the used solution.

The efficiency of the device was calculated as a ratio between the energy generated by the FC and the full (theoretical) energy that can be generated by the oxidation of hydrogen released from sodium borohydride. The amount of energy generated by the FC (4.83 kJ) was determined when pumping 10 ml of a solution containing 1 g of $NaBH_4$ into a hot reactor and a power consumption of 17 W. The oxidation energy of hydrogen is deduced from the ΔH of the reaction $H_2 + 1/2O_2 -> H_2O$, -285.83 kJ mol^{-1} H_2 [33]. So, we performed the calculation for 1 g $NaBH_4$, which corresponds to 0.05285 mol H_2 or 15.11 kJ (100% theoretical efficiency). The calculated energy efficiency of the device is 32%.

The efficiency of the studied autonomous power source is limited by the efficiency of the FC stack, which equals 40%. When it comes to commercially available FCs, their electrical energy conversion efficiency is much higher and reached 60%, with the most developed field being large-scale automobile and commercial FC vehicles in urban areas [7]. The performance of the FC is directly related to the efficiency of converting of hydrogen fuel into power. For large-scale applications, a complete utilization of hydrogen fuel is achieved, while for the small, simple design of FC utilized in the current project, because of the flushing of the H_2 supply line, a significant part of the generated H_2 gas remains unused, leading to a decrease in efficiency to 32%.

3.3. Development and design of a control system

The output voltage and current provided by the operating FC stack can vary in a broad range depending on the hydrogen flow rate, load and other operating parameters. On the other hand, it is necessary to keep the output voltage stable (12 V) regardless of the load current, and when the output current (i.e. power) changes, it is necessary to control the operation of the FC stack independently of the varying hydrogen flow and

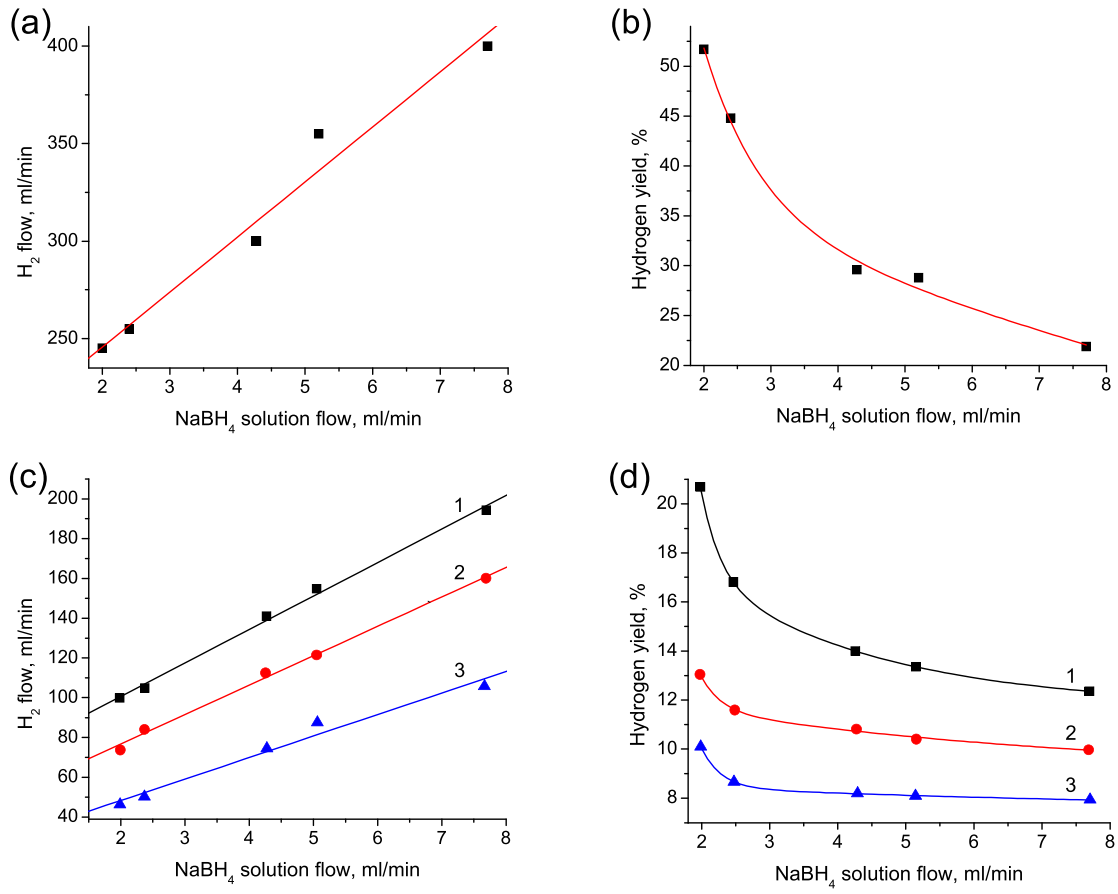

Figure 2. Effect of $NaBH_4$ solution flow rate on the hydrogen evolution rate (a), (c) and hydrogen yield (b), (d) using flat reactor with 13 mg Pt (40%)/Vulcan XC-72 catalyst on carbon cloth (a), (b) and cylindrical reactor with following catalysts: 1–100 mg Pt (40%)/Vulcan XC-72 on carbon cloth; 2–150 mg Pt on 2 g of activated carbon AG-3; 3–70 mg Pt on 5 g of titanium cramb (c), (d).

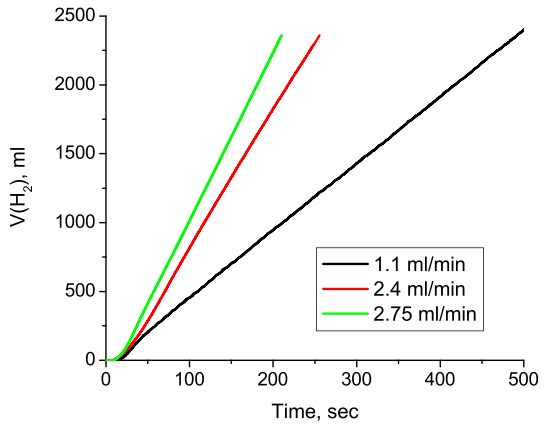

Figure 3. Time-dependent volumes of the evolved hydrogen during the hydrolysis of 10 ml of the 10% $NaBH_4$ + 5% NaOH solution in the 5 ml cylindrical flow reactor with Pt/Al_2O_3/cordierite catalyst at different rates of solution flow.

variations in the operation of the pump. To address this issue, a dedicated electronic system was developed (figure 7). The electronic control system consists of the following main components: microcontroller, voltage converter/stabilizer, battery, supercapacitor, switching elements, power supply for the electronic components and water pump, current source for charging the supercapacitor, and components for monitoring the voltage and current. The main output voltage stabilization is achieved by using a buck-boost converter, providing a constant output voltage magnitude that is either higher or lower than the input voltage. A module based on the LTC3780 chip (Analog Devices) was utilized, providing a stable 12 V output voltage in a broad input voltage range from 5 to 14 V with a high conversion efficiency.

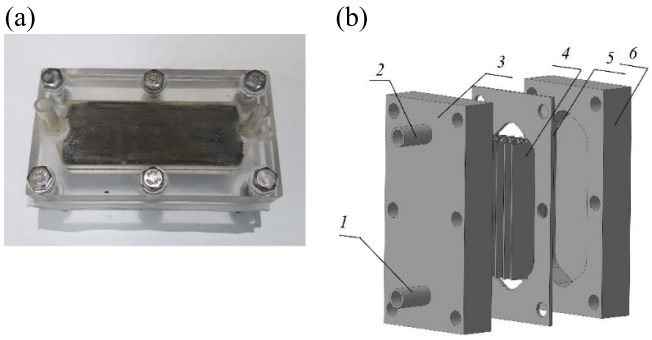

Figure 4. Overall view (a) and a structural diagram (b) of the flat flow reactor for the hydrolysis of sodium borohydride with Pt/Al_2O_3/cordierite catalyst: 1—fitting for inlet of sodium borohydride solution, 2—fitting for outlet of hydrogen and hydrolysis products, 3—reactor wall with fittings, 4—Pt/Al_2O_3/cordierite catalyst, 5—sealing silicone gasket, 6—reactor wall without fittings.

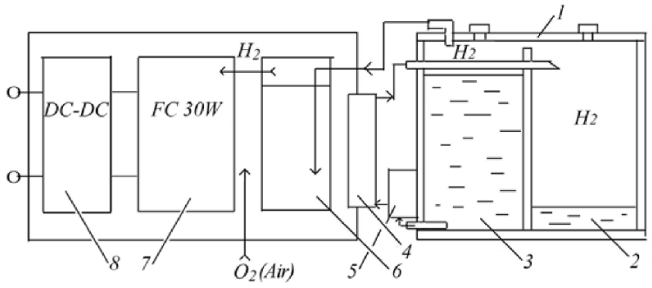

Figure 5. Schematic diagram of an autonomous power supply device: combined tank (1) with waste (2) and fresh (3) 10% $NaBH_4$ + 5% NaOH solutions; hydrolysis-type hydrogen generator with composite Pt catalyst (4); peristaltic pump (5); moisture trap (6); FC stack (7); DC-DC voltage converter-stabilizer and electronic control system (8).

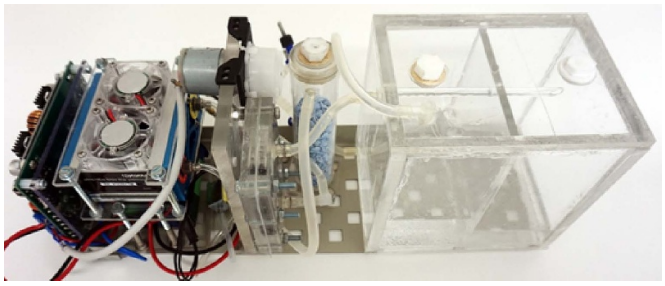

Figure 6. Prototype device for a portable energy supply.

In order to start the operation of the unit, an external power supply must be used for powering all electronic components and a peristaltic pump. For this purpose, we used a Li-ion battery with a nominal voltage of 10.8 V (0.5–2 V lower than the output voltage, 12 V). When the FC stack reaches the operation mode, the buck-boost converter starts working and then all elements of the control circuit are supplied by its 12 V output, whereas the battery is not used anymore and is disconnected. As simple and reliable switches, Schottky diodes with a low forward voltage drop were used. However, the output voltage of the FC can vary, causing occasional variations of the current. To smoothen them, a supercapacitor was used, which shows certain advantages over a battery. First of all, it has a very high ability to undergo fast charge–discharge cycles, while having a low internal resistance, and because of that it provides a good stabilization efficiency. The supercapacitor (3.2 F), which is connected to buck-boost converter input, starts charging at a constant current (~0.2 A, 1–1.5 min) just after reaching the output voltage of 12 V. After that it operates as a buffer dumping short time voltage falls from an FC stack, thus enabling smooth functioning of the buck-boost converter. Later recharging is continued by a control circuit. The control of the operating parameters as well as the measurement of the currents and voltages are performed using an EFM8BB31F32 microcontroller (Silicon Labs). It also provides the data transfer to a computer, allowing the system performance to be

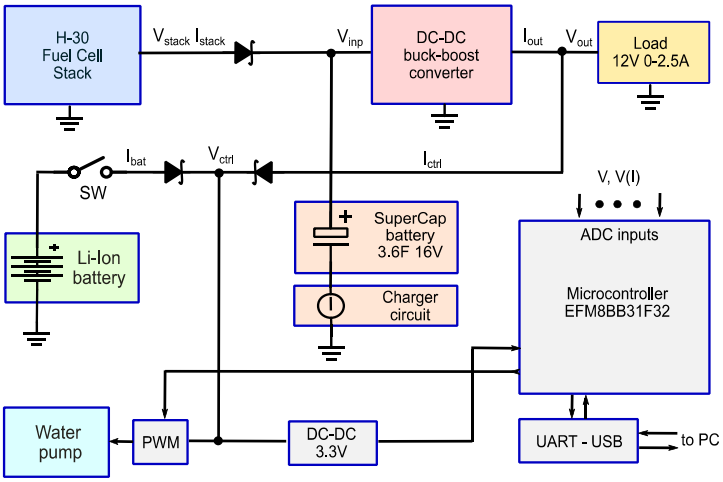

Figure 7. Block diagram of the electronic control unit.

Figure 8. The main window of the control program.

analyzed. Voltages are measured using resistive dividers and a multichannel 12-bit ADC microcontroller. For the measurements of the current, precision INA213 current-sense amplifiers (Texas Instruments) were used, and their output voltages were also measured using the ADC channels of the microcontroller. As can be seen from figure 7, the electronic control circuit (microcontroller, amplifiers, etc) is powered either by the battery (10–11 V) or by the output current at a voltage of 12 V from the point labeled Vctrl (between the Schottky diodes). The pump electric motor is also powered by this source using a transistor-based switch and a pulse width modulator (PWM) control signal from the PCA counter of the microcontroller. As supercapacitors, we used two supercapacitor battery modules, each consisting of six supercapacitors (10 F, 2.7 V), connected in series, along with a voltage-balancing circuit. The charger for a supercapacitor consists of a Power MOSFET-based constant current source (about 200 mA) with an operational amplifier. The microcontroller is powered by an additional DC-DC switch mode converter with 3.3 V output. Communication with the PC is implemented via a virtual serial port using a CP2102 (Silicon Laboratories) UART-USB bridge.

A program for data communication with the microcontroller to control the process parameters, providing data visualization and recording, was also developed. Screenshots of the working program are shown in figure 8, where typical examples of the measured performance parameters are shown. The program in real time displays the values of the measured voltages and currents of main device components (figure 7), where V_{stack} is a voltage of the FC; V_{inp} is the input voltage of the DC-DC converter; V_{out} is the output voltage on the load; V_{ctrl} is the voltage for all control circuits, which are powered either by a battery (at start-up) or by an output power (operation mode); and V_{pump} is the average (effective) voltage of the dosing pump motor powered by a PWM controlled by a microcontroller. A similar notation is used to indicate the electric current parameters.

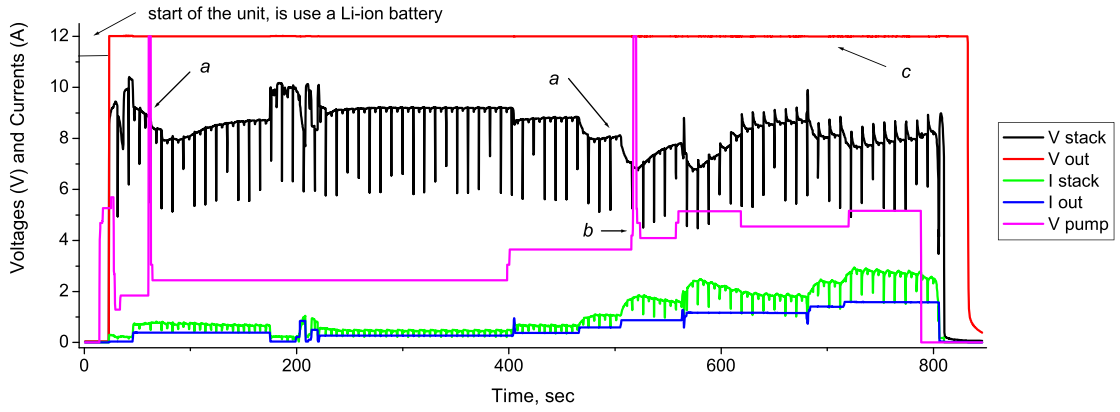

Figure 9. Voltage variations: (a) decreasing the power of the fuel cell, (b) forced by a pump (c) stabilized V_{out} of 12 V.

Figure 9 shows typical collected experimental data when monitoring the generated voltage and current characteristics, namely the output to the consumer, the FC, the dosing pump, the battery, the supercapacitor and control circuit power consumption. According to the developed algorithm of hydrogen generation, its rate is set depending on the continuous monitoring of the measured values of load current, which can change from zero to its maximum value at a full load. To increase the efficiency of the system, the hydrogen flow rate was determined experimentally and was set at the value required for the operation of an FC to provide a setpoint power. When the flow of hydrogen gas becomes too small for the operation of the FC at a given power (figure 9(a)), the pump increases the supply of aqueous solution of sodium borohydride before returning back to the optimum pumping speed (figure 9(b)). The FC performance is effectively smoothened using a supercapacitor (figure 9(c)), as its charge can maintain a power of 10 W/12 V at the load for about one minute.

The spikes in voltage and current in the operation of the device are due to the flushing of the hydrogen supply line when the hydrogen pressure exceeds the threshold set by the provider of the selected commercial 30 W H-30 PEM FC stack (FCS-B30). The supply line providing hydrogen gas to the FC has a solenoid valve, which opens releasing excess H_2 pressure until it drops back to a value close to atmospheric pressure. This results in a drop of the voltage/current/power. We have not attempted to optimize the FC performance. However, we addressed the problem by developing an electronic stabilization solution for the output voltage and current.

At the initial stage of hydrogen generation, the hydrolysis reactor warms from the starting ambient temperature to about 60 °C. This process lasts for about 2 min and the rate of the hydrolysis reaction varies even when the feed rate of the sodium borohydride solution remains unaltered. In the developed algorithm, excess hydrogen is generated in the initial stage. The measurements of the reactor temperature were not performed, and there was no control of the reaction rate when the reactor was cold. Importantly, the available excess hydrogen allows H_2 to be blown through the FC. The overpressure is maintained at about 1.5 bar using a miniature electronic valve.

When the pump voltage reaches 3 V, the amount of $NaBH_4$ solution pumped through the reactor allows the generation of 500 ml H_2 released as a result of the hydrolysis reaction. The device can stably operate from one refueling for at least 540 min.

The testing of the device's operation was carried out by repeatedly stopping and starting it. The difference between the restart of the operation and the first switch-on (when the reactor is cold) is in a shorter time of rapid pumping of the borohydride solution. In this case, the reactor is still warm, and the rate of the hydrolysis reaction is correspondingly higher (see supplementary information).

The operational specifications [34] regarding the energy requirements of the dismounted soldier have to include 10 h autonomy work (or an energy capacity of 300 Wh × h), an average power of 30 W, a volume less than 5 l, and a weight less than 3.2 kg. Taking into account the total volume (4.4 l) and weight (2.8 kg) of the pilot device, including the necessary fuel (solid $NaBH_4$) and the best operating parameters, the device can provide the required energy intensity, which is comparable with analog power systems mentioned in the literature [1, 2].

4. Summary and conclusions

An autonomous power supply device based on a 30 W FC stack and a hydrolysis-type hydrogen generator was developed. The creation of this device included the construction of a unit for hydrogen generation, testing the optimal modes of its operation, and creating an electronic control unit for the device operation. The investigation of the $NaBH_4$ hydrolysis reaction with a Pt-based catalyst depending on the reactor configuration allowed the flat type of reactor to be identified as the most suitable one. A Pt catalyst on a cordierite substrate and a 10% concentration of $NaBH_4$ solution were selected as optimal for hydrolysis, and assured the efficient operation of the 30 W FC. A Li-ion battery was used to start up the work of the developed system. An electronic control circuit of the system was developed, which regulates the hydrolysis reaction rate and hydrogen supply to the FC, and as a result, provides a variable power of the cell. An important feature of the created electronic system is the use of supercapacitors to smoothen the unstable FC operation. A Li-ion battery was used to start up the work of the developed system. These technical decisions allowed us to create the pilot device hydrolysis block—FC with a stable and continuous power supply for at least 9 h ($U_{const} = 12$ V, $I = 0$–2.5 A; nominal power = 30 W). The ratio of power to mass/volume of the developed device, when also accounting solid $NaBH_4$ as a necessary fuel, does not exceed those of the analogues described in the literature. The features of the applied electronic circuit allow stable and efficient operation to be maintained.

Data availability statement

The data that support the findings of this study are available upon reasonable request from the authors.

Acknowledgments

This work has received support from the NATO SPS Project G5233 Portable Energy Supply.

ORCID iDs

V Yartys https://orcid.org/0000-0003-4207-9127
I Zavaliy https://orcid.org/0000-0002-9825-6922

References

[1] Advanced chemical hydride-based fuel cell systems for portable military applications (Massachusetts: Protonex Technology Corporation Southborough) (Accessed 1 November 2006)
[2] Sousa C, Rangel C M, Rodrigues J C, Fernandes V R, Paiva T I and Soares D D 2010 *SPP: 3° Seminário Int. Torres Vedras* (*Portugal, 29–30 April*) pp 68–70
[3] Abdelhamid H N 2021 *Int. J. Hydrog. Energy* **46** 726–65
[4] Kozin L H, Volkov S V and Skryptun I N 2019 Modern hydrogen energetics and ecology (Kyiv: Akademperiodyka) p 364
[5] Xiao F, Yang R and Liu Z 2022 *Int. J. Hydrog. Energy* **47** 365–86
[6] Verbovytskyy Y V, Berezovets V V, Kytsya A R, Zavaliy I Y and Yartys V A 2020 *Mater. Sci.* **56** 1–14
[7] Fan L, Tu Z and Chan S H 2021 *Energy Rep.* **7** 8421–46
[8] Demirci U B, Akdim O, Andrieux J, Hannauer J, Chamoun R and Miele P 2010 *Fuel Cells* **10** 335–50
[9] Liu B H and Li Z P 2009 *J. Power Sources* **187** 527–34
[10] Muir Sean S and Yao X D 2011 *Int. J. Hydrog. Energy* **36** 5983–97
[11] Li Q and Kim H 2012 *Fuel Process. Technol.* **100** 43–48
[12] Chen B, Chen S, Bandal H A, Appiah-Ntiamoah R, Jadhav A R and Kim H 2018 *Int. J. Hydrog. Energy* **43** 9296–306
[13] Guo J, Wang B, Yang D, Wan Z, Yan P, Tian J and Yang X 2020 *Appl. Catal.* B **265** 118584
[14] Ghodke N P, Rayaprol S, Bhoraskar S V and Mathe V L 2020 *Int. J. Hydrog. Energy* **45** 16591–605
[15] Chairam S, Jarujamrus P and Amatatongchai M 2021 *J. Iran. Chem. Soc.* **18** 689–99
[16] Kytsya A, Berezovets V, Verbovytskyy Y, Bazylyak L, Kordan V, Zavaliy I and Yartys V A 2022 *J. Alloys Compd.* **908** 164484
[17] Kojima Y, Suzuki K, Fukumoto K, Kawai Y, Kimbara M, Nakanishi H and Matsumoto S 2004 *J. Power Sources* **125** 22–26
[18] Gervasio D, Tasic S and Zenhausern F 2005 *J. Power Sources* **149** 15–21
[19] Kim S J, Lee J, Kong K Y, Jung C R, Min I G, Lee S Y, Kim H J, Nam S W and Lim T H 2007 *J. Power Sources* **170** 412–8
[20] Kim K, Kim T, Lee K and Kwon S 2011 *J. Power Sources* **196** 9069–75
[21] Kim T and Kwon S 2012 *Int. J. Hydrog. Energy* **37** 615–22
[22] Pashaie P, Shakeri M and Miremadeddin R 2013 *Adv. Mat. Res.* **664** 795–800
[23] Kim J and Kim T 2014 *Energy Proc.* **61** 1992–5
[24] Kim T 2014 *Energy* **69** 721–7
[25] Lee C J and Kim T 2015 *Int. J. Hydrog. Energy* **40** 2274–82
[26] Li S C and Wang F C 2016 *Int. J. Hydrog. Energy* **41** 3038–51
[27] Kwon S, Kim M J, Kang S and Kim T 2019 *Appl. Energy* **251** 113331
[28] Kwon S, Kang M S and Kim T 2019 *Energy Proc.* **158** 1930–5

[29] Pan Z F, An L and Wen C Y 2019 *Appl. Energy* **240** 473–85
[30] Strizhak P E *et al* 2016 *Sci. Innov.* **12** 28–40
[31] Yartys V, Zavaliy I, Kytsya A, Berezovets V, Pirskyy Y, Manilevich F, Verbovytskyy Y and Lyutyy P 2021 *Hydrogen Based Energy Storage: Status and Recent Developments* ed V A Yartys, M Yu, Y I Solonin and I Y Zavaliy (Lviv: Prostir-M) pp 94–104
[32] Patil A S, Dubois T G, Sifer N, Bostic E, Gardner K, Quah M and Bolton C 2004 *J. Power Sources* **136** 220–5
[33] Dai P, Zhao X, Xu D, Wang C, Tao X, Liu X and Gao J 2019 *Int. J. Hydrog. Energy* **44** 28463–70
[34] Dean J A and Lange N A 1999 *Lange's Handbook of Chemistry* 15th edn (New York: McGraw-Hill)